Steel and Composite Structures, *Vol. 23, No. 3 (2017) 263-271*
DOI: https://doi.org/10.12989/scs.2017.23.3.263

Non-linear study of mode II delamination fracture in functionally graded beams

Victor I. Rizov *

Department of Technical Mechanics, University of Architecture, Civil Engineering and Geodesy, 1 Chr. Smirnensky blvd., 1046 – Sofia, Bulgaria

(*Received August 09, 2016, Revised December 28, 2016, Accepted January 03, 2017*)

Abstract. A theoretical study was carried-out of mode II delamination fracture behavior of the End Loaded Split (ELS) functionally graded beam configuration with considering the material non-linearity. The mechanical response of ELS was modeled analytically by using a power-law stress-strain relation. It was assumed that the material is functionally graded transversally to the beam. The non-linear fracture was investigated by using the *J*-integral approach. Equations were derived for the crack arm curvature and zero axes coordinate that are needed for the *J*-integral solution. The analysis developed is valid for a delamination crack located arbitrary along the beam height. The *J*-integral solution was verified by analyzing the strain energy release rate with considering material non-linearity. The effects of material gradient, non-linear material behavior and crack location on the fracture were evaluated. The solution derived is suitable for parametric analyses of non-linear fracture. The results obtained can be used for optimization of functionally graded beams with respect to their mode II fracture performance. Also, such simplified analytical models contribute for the understanding of delamination fracture in functionally graded beams exhibiting material non-linearity.

Keywords: functionally graded structures; fracture; material non-linearity; beam theory

1. Introduction

Functionally graded materials play an increasing important role in engineering, aerospace, nuclear energy, electronics, optics, energy conservation, etc. (Bohidar *et al*. 2014, Akbas 2015, Atmane *et al*. 2015, Bennai *et al*. 2015, Darlimaz 2015, Uslu Uysal and Kremzer 2015, Ahouel *et al*. 2016, Bedia and Bousahla 2016, Benferhat *et al*. 2016, Bounouara *et al*. 2016, Galeban *et al*. 2016, Parvanova *et al*. 2013, 2014, Uysal 2016). One of the basic advantages of functionally graded materials is that they are designed to make use of their natural or engineering functionalities in order to meet the requirements of specific material properties for different parts of a member.

The fracture mechanics study of functionally graded materials is very important for the design of devices and structures. The engineering practice indicates that fracture usually is the critical failure mode for functionally graded structures. Crack initiation and growth may drastically reduce the strength, stiffness and stability of structure (Uslu Uysal and Güven 2016) and may lead to lose of the structural capacity and functionality. It is clear that understanding of fracture behavior is vital for further development of functionally graded materials technology. Therefore, fracture of graded materials continues to attract the interest of researchers, which is reflected by the significant number of papers published in this field (Pei and Asaro 1997, Tilbrook *et al*. 2005, Carpinteri and Pugno 2006, Upadhyay and Simha 2007, Zhang *et al*. 2013).

Fracture behavior of materials with continuously graded microstructure has been studied by Pei and Assaro (1997). Fracture has been analyzed in terms of the stress intensity factors. A semi-infinite crack in an isotropic strip of a functionally graded material subjected to edge loading has been investigated by using methods of linear-elastic fracture mechanics. The solution derived has been extended to an orthotropic functionally graded strip. The effect of orthotropy on the stress intensity factors has been discussed.

Studies of cracks in functionally graded composite materials have been reviewed by Tilbrook *et al*. (2005). The influence of spatial variation of mechanical properties on the fracture behavior has been analyzed by applying linear-elastic fracture mechanics. Results of stress intensity factor calculations for cracks parallel to gradient direction have been presented. Crack propagation perpendicular to gradient has also been considered. Publications have also been reviewed in the field of fatigue fracture behavior.

Stress intensity factor analytical predictions in functionally graded materials have been reported by Carpinteri and Pugno (2006). Fracture behavior of linear-elastic plates in tension and beams under three-point bending has been investigated. Simple analytical laws have been derived that are useful in engineering applications evaluating the strength of structures composed by functionally graded materials containing re-entrant corners.

Stress intensity factor evaluation of a cracked functionally graded linear-elastic beam subjected to three-point bending has been performed by Upadhyay and Simha (2007). For this purpose, an equivalent beam of variable height has been suggested. The compliance approach has been applied. It has been shown that the equivalent beam

*Corresponding author, Professor,
E-mail: V_RIZOV_FHE@UACG.BG

ISSN: 1229-9367 (Print), 1598-6233 (Online)

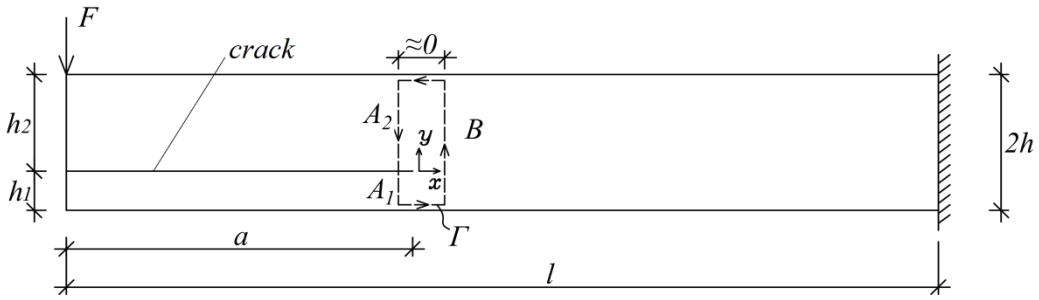

Fig. 1 The ELS beam configuration

concept can be successfully extended to carry-out engineering design analyses of fracture in beams composed of functionally graded materials.

It can be concluded that fracture analyses of functionally graded beams have been carried-out usually assuming linear-elastic material behavior. However, in reality, the stress-strain relation may be non-linear. Therefore, the present paper reports a theoretical study of delamination fracture in the functionally graded ELS beam configuration with taking into account the material non-linearity. The fracture behavior was analyzed by applying the *J*-integral approach. The effect of material gradient and crack location on the non-linear fracture was evaluated. The analysis developed holds for non-linear elastic material behavior. However, the analysis is applicable also for elastic-plastic behavior, if the external load magnitude increases only, i.e., if the beam considered undergoes active deformation (Lubliner 2006, Chakrabarty 2006). It should be mentioned that, in principle, the fracture can be studied by finite element models (Kaman and Cetisli 2012, Uslu Uysal 2017) or by analytical methods. In the present paper, the non-linear delamination fracture is studied by analytical methods since the analytical solutions are very convenient for parametric investigations of fracture in functionally graded beams which exhibit non-linear behavior of material.

2. Fracture study with taking into account the material non-linearity

The ELS functionally graded beam under consideration is shown schematically in Fig. 1. It was assumed that the material is functionally graded transversely to the beam. There is a delamination crack of length a (it should be noted that the present study was motivated also by the fact that functionally graded materials can be built up layer by layer (Bohidar *et al*. 2014), which is a premise for appearance of delamination cracks between layers). The crack is located arbitrary along the beam height (Fig. 1), i.e., the ELS configuration is asymmetrical (the lower and upper crack arm thicknesses are h_1 and h_2, respectively). The right-hand end of beam is clamped. One ransverse force, F, is applied at the beam free end. The beam cross-section is a rectangle of width, b, and height, $2h$.

The non-linear fracture behavior was analyzed by using the *J*-integral approach for functionally graded materials (Anlas *et al*. 2000, Rajabi *et al*. 2016). The *J*-integral was written as

$$J = \int_{\Gamma}\left[u_0 \cos\alpha - \left(p_x \frac{\partial u}{\partial x} + p_y \frac{\partial v}{\partial x}\right)\right]ds - \int_{A} \frac{\partial u_0}{\partial x} q dA, \quad (1)$$

where Γ is a contour of integration going from the lower crack face to the upper crack face in the counter clockwise direction, u_0 is the strain energy density, α is the angle between the outwards normal vector to the contour of integration and the crack direction, p_x and p_y are the components of stress vector, u and v are the components of displacement vector with respect to the crack tip coordinate system xy (x is directed along the crack), ds is a differential element along the contour, A is the area enclosed by that contour, q is a weight function with a value of unity at the crack tip, zero along the contour and arbitrary elsewhere. It should be specified that the partial derivative $\partial u_0 / \partial x$ exists only if the material property is an explicit function of x (Anlas *et al*. 2000).

The *J*-integral was solved by using an integration contour, Γ, that consists of the ELS beam cross-sections ahead and behind the crack tip as illustrated in Fig. 1. The integration contour has three segments (A_1, A_2, and B). The *J*-integral solution was obtained by summation

$$J = J_{A_1} + J_{A_2} + J_B, \quad (2)$$

where J_{A_1}, J_{A_2} and J_B are the values in segments A_1, A_2 and

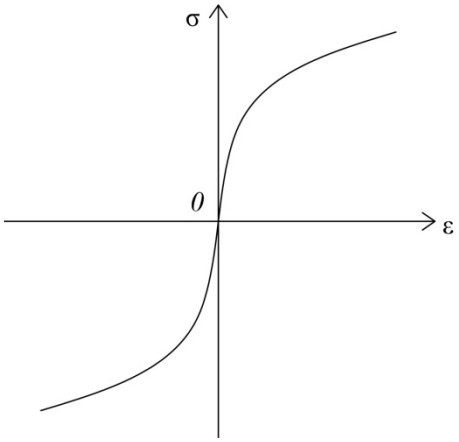

Fig. 2 Non-linear stress-strain curve

B, respectively. Integration contour segments A_1 and A_2 are defined by the cross-sections of lower and upper crack arm behind the crack tip. Segment B is defined by the beam cross-section ahead of the crack tip (Fig. 1).

It was assumed that the mechanical response of functionally graded ELS beam configuration can be described by a power-law stress-strain relation (Petrov 2014)

$$\sigma = H\varepsilon^{m_1}, \tag{3}$$

where σ is the stress, ε is the strain, H and m_1 are material properties. The tensile and compressive behaviors are identical as shown in Fig. 2. The present analysis was based on the small strain assumption (it should be noted that this assumption has been frequently used in fracture analyses of functionally graded materials (Pei and Asaro 1997, Carpinteri and Pugno 2006, Upadhyay and Simha 2007)). Besides, it was assumed that the value of H varies linearly along the beam height from H_0 in the upper edge to H_1 in the lower edge of beam (i.e., the material is functionally graded along the ELS beam height). Thus, H was written as

$$H = H_0 + \frac{H_1 - H_0}{2h}(h + z_3), \tag{4}$$

where the z_3–axis originates from the beam cross-section centre and is directed downwards.

The curvature of lower and upper crack arm in the cross-section behind the crack tip is needed in order to obtain the J-integral solutions in segments A_1 and A_2. The fact that the curvatures of crack arms in the ELS beam are equal was used to determine the curvature. It was written

$$\kappa_1 = \kappa_2, \tag{5}$$

where, κ_1 and κ_2 are the curvatures of lower and upper crack arm, respectively.

The crack arm curvature was determined in the following way. First, the equations of equilibrium of lower crack arm cross-section were written as

$$N_1 = \int_{-\frac{h_1}{2}}^{\frac{h_1}{2}} \sigma(\varepsilon) b dz_1 = 0, \tag{6}$$

$$M_1 = \int_{-\frac{h_1}{2}}^{\frac{h_1}{2}} \sigma(\varepsilon) b z_1 dz_1, \tag{7}$$

where N_1 and M_1 are the axial force and bending moment in the lower crack arm behind the crack tip, respectively (obviously, $N_1 = 0$).

It was assumed that the Bernoulli's hypothesis for plane sections is applicable, since the span to height ratio for the beam considered is large. (It should be mentioned that the Bernoulli's hypothesis for plane sections has been widely applied when analyzing fracture in functionally graded beams (Pei and Asaro 1997, Carpinteri and Pugno 2006, Upadhyay and Simha 2007). Thus, the strain, ε, was written as

$$\varepsilon = \kappa_1 (z_1 - z_{1n_1}), \tag{8}$$

where z_{1n_1} is the neutral axis coordinate (the neutral axis shifts from the centroid, since the material is functionally graded along the beam height).

The variation of H along the lower crack arm cross-section height was expressed as (refer to Eq. (4))

$$H = H_0^L + \frac{H_1 - H_0^L}{h_1}\left(\frac{h_1}{2} + z_1\right), \tag{9}$$

where

$$H_0^L = H_0 + \frac{H_1 - H_0}{2h}(2h - h_1) \tag{10}$$

is the value of H in the upper edge of the lower crack arm.

After substitution of Eqs. (3), (8) and (9) in Eqs. (6) and (7) and solving the integrals, we obtained

$$\begin{aligned} &\frac{1}{m_1+1}\left[\frac{1}{2}\left(H_0^L + H_1\right) + \frac{1}{h_1}\left(H_1 - H_0^L\right) z_{1n_1}\right] \\ &\left[\left(\frac{h_1}{2} - z_{1n_1}\right)^{m_1+1} - \left(-\frac{h_1}{2} - z_{1n_1}\right)^{m_1+1}\right] \\ &+ \frac{1}{h_1}\left(H_1 - H_0^L\right)\frac{1}{m_1+2}\left[\left(\frac{h_1}{2} - z_{1n_1}\right)^{m_1+2} - \left(-\frac{h_1}{2} - z_{1n_1}\right)^{m_1+2}\right] = 0, \end{aligned} \tag{11}$$

$$\begin{aligned} M_1 = \kappa_1^{m_1} b \Bigg\{ & H_0^L \Bigg\{ \frac{1}{m_1+2}\left[\left(\frac{h_1}{2} - z_{1n_1}\right)^{m_1+2} - \left(-\frac{h_1}{2} - z_{1n_1}\right)^{m_1+2}\right] \\ & + \frac{1}{m_1+1}\left[\left(\frac{h_1}{2} - z_{1n_1}\right)^{m_1+1} z_{1n_1} - \left(-\frac{h_1}{2} - z_{1n_1}\right)^{m_1+1} z_{1n_1}\right]\Bigg\} \\ & + \frac{1}{2}\left(H_1 - H_0^L\right)\Bigg\{ \frac{1}{m_1+2}\left[\left(\frac{h_1}{2} - z_{1n_1}\right)^{m_1+2} - \left(-\frac{h_1}{2} - z_{1n_1}\right)^{m_1+2}\right] \\ & + \frac{z_{1n_1}}{m_1+1}\left[\left(\frac{h_1}{2} - z_{1n_1}\right)^{m_1+1} - \left(-\frac{h_1}{2} - z_{1n_1}\right)^{m_1+1}\right]\Bigg\} \\ & + \frac{1}{h_1}\left(H_1 - H_0^L\right)\Bigg\{ \frac{1}{m_1+3}\left[\left(\frac{h_1}{2} - z_{1n_1}\right)^{m_1+3} - \left(-\frac{h_1}{2} - z_{1n_1}\right)^{m_1+3}\right] \\ & + \frac{2z_{1n_1}}{m_1+2}\left[\left(\frac{h_1}{2} - z_{1n_1}\right)^{m_1+2} - \left(-\frac{h_1}{2} - z_{1n_1}\right)^{m_1+2}\right] \\ & + \frac{z_{1n_1}^2}{m_1+1}\left[\left(\frac{h_1}{2} - z_{1n_1}\right)^{m_1+1} - \left(-\frac{h_1}{2} - z_{1n_1}\right)^{m_1+1}\right]\Bigg\}\Bigg\}. \end{aligned} \tag{12}$$

It is obvious that at $m_1 = 1$ the non-linear stress-strain relation Eq. (3) transforms into the Hooke's law. This means that at $m_1 = 1$ Eq. (12) should transform in the formula for curvature of linear-elastic beam. Indeed, by substitution of $m_1 = 1$ and $H_1 = H_0 = E$ (E is the modulus of elasticity) in Eq. (12), we obtained

$$\kappa_1 = \frac{12M_1}{Eb h_1^3}, \tag{13}$$

which is the known formula for the curvature of linear-elastic homogeneous beams.

The neutral axis coordinate, z_{1n_1}, can be obtained from (11). For this purpose, (11) should be solved with respect to z_{1n_1} by using the MatLab computer program. Then z_{1n_1} can be substituted in Eq. (12). In this way, the number of unknowns in Eq. (12) can be reduced to two (M_1 and κ_1). By considering the equilibrium of upper crack arm, two equations identical with Eqs. (11) and (12) were written

$$\begin{aligned}&\frac{1}{m_1+1}\left[\frac{1}{2}\left(H_0+H_0^L\right)+\frac{1}{h_2}\left(H_0^L-H_0\right)z_{2n_2}\right]\\&\left[\left(\frac{h_2}{2}-z_{2n_2}\right)^{m_1+1}-\left(-\frac{h_2}{2}-z_{2n_2}\right)^{m_1+1}\right]+\\&+\frac{1}{h_2}\left(H_0^L-H_0\right)\frac{1}{m_1+2}\left[\left(\frac{h_2}{2}-z_{2n_2}\right)^{m_1+2}-\left(-\frac{h_2}{2}-z_{2n_2}\right)^{m_1+2}\right]=0,\end{aligned}\tag{14}$$

$$\begin{aligned}M_1=M-\kappa_1^{m_1}b\Bigg\{&H_0\Bigg\{\frac{1}{m_1+2}\left[\left(\frac{h_2}{2}-z_{2n_2}\right)^{m_1+2}-\left(-\frac{h_2}{2}-z_{2n_2}\right)^{m_1+2}\right]\\&+\frac{1}{m_1+1}\left[\left(\frac{h_2}{2}-z_{2n_2}\right)^{m_1+1}z_{2n_2}-\left(-\frac{h_2}{2}-z_{2n_2}\right)^{m_1+1}z_{2n_2}\right]\Bigg\}\\&+\frac{1}{2}\left(H_0^L-H_0\right)\Bigg\{\frac{1}{m_1+2}\left[\left(\frac{h_2}{2}-z_{2n_2}\right)^{m_1+2}-\left(-\frac{h_2}{2}-z_{2n_2}\right)^{m_1+2}\right]\\&+\frac{z_{2n_2}}{m_1+1}\left[\left(\frac{h_2}{2}-z_{2n_2}\right)^{m_1+1}-\left(-\frac{h_2}{2}-z_{2n_2}\right)^{m_1+1}\right]\Bigg\}\\&+\frac{1}{h_2}\left(H_0^L-H_0\right)\Bigg\{\frac{1}{m_1+3}\left[\left(\frac{h_2}{2}-z_{2n_2}\right)^{m_1+3}-\left(-\frac{h_2}{2}-z_{2n_2}\right)^{m_1+3}\right]\\&+\frac{2z_{2n_2}}{m_1+2}\left[\left(\frac{h_2}{2}-z_{2n_2}\right)^{m_1+2}-\left(-\frac{h_2}{2}-z_{2n_2}\right)^{m_1+2}\right]\\&+\frac{z_{2n_2}^2}{m_1+1}\left[\left(\frac{h_2}{2}-z_{2n_2}\right)^{m_1+1}-\left(-\frac{h_2}{2}-z_{2n_2}\right)^{m_1+1}\right]\Bigg\}\Bigg\},\end{aligned}\tag{15}$$

where z_{2n_2} is the neutral axis coordinate of upper crack arm cross-section, H_0 and H_0^L are the values of H in the upper and lower edge of upper crack arm, respectively (H_0^L is determined by Eq. (10)). It should be noted that dependence Eq. (5) was taken into account in Eq. (15). Also, in Eq. (15), the bending moment, M_2, in the cross-section of upper crack arm behind the crack tip was replaced with $M - M_1$, where M is crack tip cross-sectional bending moment in the ELS beam (Fig. 1). The neutral axis coordinate, z_{2n_2}, can be obtained from Eq. (14) by using the MatLab computer program and substituted in Eq. (15). In this way, the number of unknowns in (15) can be reduced to two (M_1 and κ_1). Then, by combining Eqs. (12) and (15), the unknowns M_1 and κ_1 were determined as

$$M_1=\frac{M\psi_1}{\psi_1+\psi_2},\tag{16}$$

$$\kappa_1=\left(\frac{M\psi_1^2}{\psi_1+\psi_2}\right)^{\frac{1}{m_1}},\tag{17}$$

where

$$\begin{aligned}\psi_1=b\Bigg\{&H_0^L\Bigg\{\frac{1}{m_1+2}\left[\left(\frac{h_1}{2}-z_{1n_1}\right)^{m_1+2}-\left(-\frac{h_1}{2}-z_{1n_1}\right)^{m_1+2}\right]\\&+\frac{1}{m_1+1}\left[\left(\frac{h_1}{2}-z_{1n_1}\right)^{m_1+1}z_{1n_1}-\left(-\frac{h_1}{2}-z_{1n_1}\right)^{m_1+1}z_{1n_1}\right]\Bigg\}\\&+\frac{1}{2}\left(H_1-H_0^L\right)\Bigg\{\frac{1}{m_1+2}\left[\left(\frac{h_1}{2}-z_{1n_1}\right)^{m_1+2}-\left(-\frac{h_1}{2}-z_{1n_1}\right)^{m_1+2}\right]\\&+\frac{z_{1n_1}}{m_1+1}\left[\left(\frac{h_1}{2}-z_{1n_1}\right)^{m_1+1}-\left(-\frac{h_1}{2}-z_{1n_1}\right)^{m_1+1}\right]\Bigg\}\\&+\frac{1}{h_1}\left(H_1-H_0^L\right)\Bigg\{\frac{1}{m_1+3}\left[\left(\frac{h_1}{2}-z_{1n_1}\right)^{m_1+3}-\left(-\frac{h_1}{2}-z_{1n_1}\right)^{m_1+3}\right]\\&+\frac{2z_{1n_1}}{m_1+2}\left[\left(\frac{h_1}{2}-z_{1n_1}\right)^{m_1+2}-\left(-\frac{h_1}{2}-z_{1n_1}\right)^{m_1+2}\right]\\&+\frac{z_{1n_1}^2}{m_1+1}\left[\left(\frac{h_1}{2}-z_{1n_1}\right)^{m_1+1}-\left(-\frac{h_1}{2}-z_{1n_1}\right)^{m_1+1}\right]\Bigg\}\Bigg\},\end{aligned}\tag{18}$$

$$\begin{aligned}\psi_2=b\Bigg\{&H_0\Bigg\{\frac{1}{m_1+2}\left[\left(\frac{h_2}{2}-z_{2n_2}\right)^{m_1+2}-\left(-\frac{h_2}{2}-z_{2n_2}\right)^{m_1+2}\right]\\&+\frac{1}{m_1+1}\left[\left(\frac{h_2}{2}-z_{2n_2}\right)^{m_1+1}z_{2n_2}-\left(-\frac{h_2}{2}-z_{2n_2}\right)^{m_1+1}z_{2n_2}\right]\Bigg\}\\&+\frac{1}{2}\left(H_0^L-H_0\right)\Bigg\{\frac{1}{m_1+2}\left[\left(\frac{h_2}{2}-z_{2n_2}\right)^{m_1+2}-\left(-\frac{h_2}{2}-z_{2n_2}\right)^{m_1+2}\right]\\&+\frac{z_{2n_2}}{m_1+1}\left[\left(\frac{h_2}{2}-z_{2n_2}\right)^{m_1+1}-\left(-\frac{h_2}{2}-z_{2n_2}\right)^{m_1+1}\right]\Bigg\}\\&+\frac{1}{h_2}\left(H_0^L-H_0\right)\Bigg\{\frac{1}{m_1+3}\left[\left(\frac{h_2}{2}-z_{2n_2}\right)^{m_1+3}-\left(-\frac{h_2}{2}-z_{2n_2}\right)^{m_1+3}\right]\\&+\frac{2z_{2n_2}}{m_1+2}\left[\left(\frac{h_2}{2}-z_{2n_2}\right)^{m_1+2}-\left(-\frac{h_2}{2}-z_{2n_2}\right)^{m_1+2}\right]\\&+\frac{z_{2n_2}^2}{m_1+1}\left[\left(\frac{h_2}{2}-z_{2n_2}\right)^{m_1+1}-\left(-\frac{h_2}{2}-z_{2n_2}\right)^{m_1+1}\right]\Bigg\}\Bigg\}.\end{aligned}\tag{19}$$

After that, the bending moment in the upper crack arm can be calculated as

$$M_2=M-M_1.\tag{20}$$

It should be noted that after substitution of $m_1 = 1$ and $H_1 = H_0 = E$ in Eqs. (12) and (15) the curvature, κ_1, and bending moments, M_1 and M_2, were obtained from Eqs. (16), (17) and (20) as

$$\kappa_1=\frac{12M}{Eb\left(h_1^3+h_2^3\right)},\tag{21}$$

$$M_1=M\frac{h_1^3}{h_1^3+h_2^3},\tag{22}$$

$$M_2=M\frac{h_2^3}{h_1^3+h_2^3}.\tag{23}$$

Eqs. (21), (22) and (23) coincide with the known formulae for curvature and bending moments in combined linear-elastic homogeneous beams.

The solution of *J*-integral in segment A_1 of the integration contour (Fig. 1) was obtained in the following way. The components of *J*-integral were written as

$$\begin{aligned} p_x &= -\sigma = -H\varepsilon^{m_1}, \qquad p_y = 0, \\ \cos\alpha &= -1, \qquad ds = dz_1, \end{aligned} \tag{24}$$

where the coordinate, z_1, varies in the interval $[-h_1/2, h_1/2]$. Fig. 3 illustrates the distribution of stresses in segment A_1. Partial derivative, $\partial u_0 / \partial x$, in the *J*-integral Eq. (1) was written as

$$\frac{\partial u_0}{\partial x} = 0, \tag{25}$$

since the strain energy density does not depend explicitly on x (the material property H is not a function of x, because the material is functionally graded transversally to the beam only (refer to Eq. (4)).

Partial derivative, $\partial u / \partial x$, in Eq. (1) was obtained as

$$\frac{\partial u}{\partial x} = \varepsilon = \kappa_1 \left(z_1 - z_{1n_1} \right), \tag{26}$$

where κ_1 and z_{1n_1} were found from Eqs. (11), (12), (14) and (17) (the coordinate, z_1, is shown in Fig. 3).

The strain energy density, u_0, is equal to the area *OPQ* enclosed by the stress-strain curve (Fig. 4). Thus

$$u_0 = \int_0^{\varepsilon} \sigma(\varepsilon) d\varepsilon. \tag{27}$$

By substitution of Eq. (3) in Eq. (27), it was obtained

$$u_0 = \frac{H\varepsilon^{m_1+1}}{m_1+1}. \tag{28}$$

After substitution of Eqs. (8), (9), (24), (25), (26) and (28) in Eq. (1), the *J*-integral solution in segment A_1 was found as

$$\begin{aligned} J_{A_1} &= \frac{\kappa_1^{m_1+1} H_0^L}{(m_1+1)(m_1+2)} \left[\left(-\frac{h_1}{2} - z_{1n_1} \right)^{m_1+2} - \left(\frac{h_1}{2} - z_{1n_1} \right)^{m_1+2} \right] \\ &+ \frac{\kappa_1^{m_1+1} \left(H_1 - H_0^L \right)}{m_1+1} \left\{ \frac{1}{2(m_1+2)} \left[\left(-\frac{h_1}{2} - z_{1n_1} \right)^{m_1+2} - \left(\frac{h_1}{2} - z_{1n_1} \right)^{m_1+2} \right] \right. \\ &+ \frac{1}{h_1(m_1+3)} \left[\left(-\frac{h_1}{2} - z_{1n_1} \right)^{m_1+3} - \left(\frac{h_1}{2} - z_{1n_1} \right)^{m_1+3} \right] \\ &\left. + \frac{z_{1n_1}}{h_1(m_1+2)} \left[\left(-\frac{h_1}{2} - z_{1n_1} \right)^{m_1+2} - \left(\frac{h_1}{2} - z_{1n_1} \right)^{m_1+2} \right] \right\} \\ &+ \kappa_1^{m_1+1} \left\{ \frac{H_0^L}{m_1+2} \left[\left(\frac{h_1}{2} - z_{1n_1} \right)^{m_1+2} - \left(-\frac{h_1}{2} - z_{1n_1} \right)^{m_1+2} \right] \right. \\ &+ \frac{H_1 - H_0^L}{2(m_1+2)} \left[\left(\frac{h_1}{2} - z_{1n_1} \right)^{m_1+2} - \left(-\frac{h_1}{2} - z_{1n_1} \right)^{m_1+2} \right] \\ &+ \frac{H_1 - H_0^L}{h_1(m_1+3)} \left[\left(\frac{h_1}{2} - z_{1n_1} \right)^{m_1+3} - \left(-\frac{h_1}{2} - z_{1n_1} \right)^{m_1+3} \right] \\ &\left. + \frac{z_{1n_1} \left(H_1 - H_0^L \right)}{h_1(m_1+2)} \left[\left(\frac{h_1}{2} - z_{1n_1} \right)^{m_1+2} - \left(-\frac{h_1}{2} - z_{1n_1} \right)^{m_1+2} \right] \right\}. \end{aligned} \tag{29}$$

The solution of *J*-integral in segment A_2 of the integration contour (Fig. 1) was found again by Eq. (29). For this purpose, h_1 and z_{1n_1} were replaced with h_2 and z_{2n_2}, respectively. Besides, H_0^L and H_1 were replaced with H_0 and H_0^L, respectively (H_0^L was determined by Eq. (10)). Thus, the solution was written as

$$\begin{aligned} J_{A_2} &= \frac{\kappa_1^{m_1+1} H_0}{(m_1+1)(m_1+2)} \left[\left(-\frac{h_2}{2} - z_{2n_2} \right)^{m_1+2} - \left(\frac{h_2}{2} - z_{2n_2} \right)^{m_1+2} \right] \\ &+ \frac{\kappa_1^{m_1+1} \left(H_0^L - H_0 \right)}{m_1+1} \left\{ \frac{1}{2(m_1+2)} \left[\left(-\frac{h_2}{2} - z_{2n_2} \right)^{m_1+2} - \left(\frac{h_2}{2} - z_{2n_2} \right)^{m_1+2} \right] \right. \\ &+ \frac{1}{h_1(m_1+3)} \left[\left(-\frac{h_2}{2} - z_{2n_2} \right)^{m_1+3} - \left(\frac{h_2}{2} - z_{1n_1} \right)^{m_1+3} \right] \\ &\left. + \frac{z_{2n_2}}{h_1(m_1+2)} \left[\left(-\frac{h_2}{2} - z_{2n_2} \right)^{m_1+2} - \left(\frac{h_2}{2} - z_{2n_2} \right)^{m_1+2} \right] \right\} \\ &+ \kappa_1^{m_1+1} \left\{ \frac{H_0}{m_1+2} \left[\left(\frac{h_2}{2} - z_{2n_2} \right)^{m_1+2} - \left(-\frac{h_2}{2} - z_{2n_2} \right)^{m_1+2} \right] \right. \\ &+ \frac{H_0^L - H_0}{2(m_1+2)} \left[\left(\frac{h_2}{2} - z_{2n_2} \right)^{m_1+2} - \left(-\frac{h_2}{2} - z_{2n_2} \right)^{m_1+2} \right] \\ &+ \frac{H_0 - H_0}{h_1(m_1+3)} \left[\left(\frac{h_2}{2} - z_{2n_2} \right)^{m_1+3} - \left(-\frac{h_2}{2} - z_{2n_2} \right)^{m_1+3} \right] \\ &\left. + \frac{z_{2n_2} \left(H_0^L - H_0 \right)}{h_2(m_1+2)} \left[\left(\frac{h_2}{2} - z_{2n_2} \right)^{m_1+2} - \left(-\frac{h_2}{2} - z_{2n_2} \right)^{m_1+2} \right] \right\}, \end{aligned} \tag{30}$$

where z_{2n_2} was found from Eq. (14).

The *J*-integral components in segment *B* of the integration contour (Fig. 1) were written as

$$p_x = \sigma = H\varepsilon^{m_1}, \qquad p_y = 0, \tag{31}$$

$$\cos\alpha = 1, \qquad ds = -dz_3, \tag{32}$$

$$\frac{\partial u_0}{\partial x} = 0, \qquad \varepsilon = \kappa_3 (z_3 - z_{3n_3}). \tag{33}$$

Eqs. (11) and (12) were used to obtain the ELS beam curvature, κ_3, and neutral axis coordinate, z_{3n_3}, in the cross-section ahead of the crack tip. For this purpose, M_1, h_1, κ_1, z_{1n_1} and H_0^L were replaced with M, $2h$, κ_3, z_{3n_3} and H_0, respectively. Eq. (11) can be solved with respect to z_{3n_3} by using the MatLab computer program. Then, z_{3n_3} can be substituted in Eq. (12). After that, the curvature, κ_3, was determined from Eq. (12) as

$$\kappa_3 = \left(\frac{M}{\varphi} \right)^{\frac{1}{m_1}}, \tag{34}$$

where

$$\varphi = b\left\{H_0\left\{\frac{1}{m_1+2}\left[\left(h-z_{3n_3}\right)^{m_1+2}-\left(-h-z_{3n_3}\right)^{m_1+2}\right]\right.\right.$$
$$+\frac{1}{m_1+1}\left[\left(h-z_{3n_3}\right)^{m_1+1}z_{3n_3}-\left(-h-z_{3n_3}\right)^{m_1+1}z_{3n_3}\right]\Big\}$$
$$+\frac{1}{2}\left(H_1-H_0\right)\left\{\frac{1}{m_1+2}\left[\left(h-z_{3n_3}\right)^{m_1+2}-\left(-h-z_{3n_3}\right)^{m_1+2}\right]\right.$$
$$\left.+\frac{z_{3n_3}}{m_1+1}\left[\left(h-z_{3n_3}\right)^{m_1+1}-\left(-h-z_{3n_3}\right)^{m_1+1}\right]\right\} \quad (35)$$
$$+\frac{1}{h_1}\left(H_1-H_0\right)\left\{\frac{1}{m_1+3}\left[\left(h-z_{3n_3}\right)^{m_1+3}-\left(-h-z_{3n_3}\right)^{m_1+3}\right]\right.$$
$$+\frac{2z_{3n_3}}{m_1+2}\left[\left(h-z_{3n_3}\right)^{m_1+2}-\left(-h-z_{3n_3}\right)^{m_1+2}\right]$$
$$\left.\left.+\frac{z_{3n_3}^2}{m_1+1}\left[\left(h-z_{3n_3}\right)^{m_1+1}-\left(-h-z_{3n_3}\right)^{m_1+1}\right]\right\}\right\}$$

The partial derivative was found as

$$\frac{\partial u}{\partial x}=\kappa_3\left(z_3-z_{3n_3}\right). \quad (36)$$

The *J*-integral solution in segment *B* of the integration contour was obtained after substitution of Eqs. (4), (28), (31), (32), (33) and (36) in Eq. (1)

$$J_B=-\frac{\kappa_3^{m_1+1}H_0}{\left(m_1+1\right)\left(m_1+2\right)}\left[\left(-h-z_{3n_3}\right)^{m_1+2}-\left(h-z_{3n_3}\right)^{m_1+2}\right]$$
$$-\frac{\kappa_3^{m_1+1}\left(H_1-H_0\right)}{m_1+1}\left\{\frac{1}{2\left(m_1+2\right)}\left[\left(-h-z_{3n_3}\right)^{m_1+2}-\left(h-z_{3n_3}\right)^{m_1+2}\right]\right.$$
$$+\frac{1}{2h\left(m_1+3\right)}\left[\left(-h-z_{3n_3}\right)^{m_1+3}-\left(h-z_{3n_3}\right)^{m_1+3}\right]$$
$$\left.+\frac{z_{3n_3}}{2h\left(m_1+2\right)}\left[\left(-h-z_{3n_3}\right)^{m_1+2}-\left(h-z_{3n_3}\right)^{m_1+2}\right]\right\} \quad (37)$$
$$-\kappa_3^{m_1+1}\left\{\frac{H_0}{m_1+2}\left[\left(h-z_{3n_3}\right)^{m_1+2}-\left(-h-z_{3n_3}\right)^{m_1+2}\right]\right.$$
$$+\frac{H_1-H_0}{2\left(m_1+2\right)}\left[\left(h-z_{3n_3}\right)^{m_1+2}-\left(-h-z_{3n_3}\right)^{m_1+2}\right]$$
$$+\frac{H_1-H_0}{2h\left(m_1+3\right)}\left[\left(h-z_{3n_3}\right)^{m_1+3}-\left(-h-z_{3n_3}\right)^{m_1+3}\right]$$
$$\left.+\frac{z_{3n_3}\left(H_1-H_0\right)}{2h\left(m_1+2\right)}\left[\left(h-z_{3n_3}\right)^{m_1+2}-\left(-h-z_{3n_3}\right)^{m_1+2}\right]\right\}$$

The *J*-integral final non-linear solution was found by substitution of Eqs. (29), (30) and (37) in Eq. (2). The formula obtained is not reported here, because it is cumbersome.

It should be noted that by substitution of $m_1 = 1$, $H_1 = H_0 = E$ and $h_1 = h_2 = h$ in Eqs. (29), (30), (37) and (2), we found

$$J=\frac{9M^2}{4Eb^2h^3}, \quad (38)$$

which coincides with the formula for strain energy release rate, when the crack is located in the mid-plane of linear-elastic homogeneous ELS beam (Szekrenyes 2012).

The *J*-integral non-linear solution derived was verified by analyzing the strain energy release rate, *G*, in the functionally graded ELS beam with taking into account the non-linear material behavior. For this purpose, a small crack length increase, Δa, was given (the external loading was kept constant). The strain energy release rate associated with Δa was written as

$$G=\frac{\Delta W_{ext}-\Delta U}{\Delta A_a}, \quad (39)$$

where ΔW_{ext} and ΔU are the changes of external work and strain energy, respectively. The crack area increase was expressed as

$$\Delta A_a = b\Delta a. \quad (40)$$

The change of external work was obtained as

$$\Delta W_{ext}=\Delta U^*+\Delta U, \quad (41)$$

where ΔU^* is the change of the complimentary strain energy. By combining of Eqs. (39) and (41), we derived

$$G=\frac{\Delta U^*}{\Delta A_a}, \quad (42)$$

where

$$\Delta U^*=U_b^*-U_a^*. \quad (43)$$

In Eq. (43), U_b^* and U_a^* are the complimentary strain energies before and after the increase of crack, respectively. By substitution of Eqs. (40) and (43) in Eq. (42), we obtained

$$G=\frac{U_a^*-U_b^*}{b\Delta a}. \quad (44)$$

The complimentary strain energy before the increase of crack was calculated as

$$U_b^*=\Delta ab\int_{-h}^{h}u_0^*dz_3, \quad (45)$$

where the complimentary strain energy density, u_0^*, in Eq. (45) is equal to the area *OQR* that supplements the area *OPQ* enclosed by the stress-strain curve to a rectangle (Fig. 4). Therefore, the complimentary strain energy density was written as

$$u_0^*=\sigma\varepsilon-u_0, \quad (46)$$

where the strain energy density, u_0, was found by Eq. (28).

The complimentary strain energy after the increase of crack was written as

$$U_a^*=U_{a_1}^*+U_{a_2}^* \quad (47)$$

where

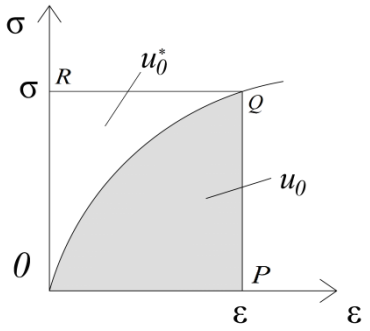

Fig. 4 Strain energy density, u_0, and complimentary strain energy density, u_0^*

$$U_{a_1}^* = \Delta ab \int_{-\frac{h_1}{2}}^{\frac{h_1}{2}} u_0^* dz_1 \tag{48}$$

and

$$U_{a_2}^* = \Delta ab \int_{-\frac{h_2}{2}}^{\frac{h_2}{2}} u_0^* dz_2 \tag{49}$$

are the complimentary strain energies in the lower and in upper crack arm, respectively. By combining of Eqs. (44), (45), (47), (48) and (49), we derived

$$G = \int_{-\frac{h_1}{2}}^{\frac{h_1}{2}} u_0^* dz_1 + \int_{-\frac{h_2}{2}}^{\frac{h_2}{2}} u_0^* dz_2 - \int_{-h}^{h} u_0^* dz_3 \tag{50}$$

Finally, by substitution of Eqs. (3), (4), (8), (9), (10) and (28) in Eq. (50), we obtained the formula for strain energy release rate that is exact match of the *J*-integral non-linear solution. This fact is a verification of the non-linear fracture analysis of functionally graded ELS beam configuration developed in the present paper.

3. Parametric analyses

Parametric analyses were performed in order to evaluate effects of material gradient, H_1/H_0 (refer to Eq. (4)) and material non-linearity on the fracture behavior of functionally graded ELS beam configuration. For this purpose, calculations were carried-out by using the *J*-integral non-linear solution obtained in the present paper. In these calculations, it was assumed that F = 15 N, b = 0.02 m, h = 0.003 m, a = 0.09 m and m_1 = 0.7. It should be specified that H_0 was kept constant in the calculations. Thus, H_1 was varied in order to achieve various H_1/H_0 ratios. The *J*-integral values generated by the calculations were presented in non-dimensional form by using the formula $J_N = J/(H_0 b)$). The results of these calculations were shown in Fig. 5 where the *J*-integral value was plotted against H_1/H_0 ratio for $h_1/2h$ = 0.5. The diagrams in Fig. 5 indicate that the *J*-integral value decreases with increasing H_1/H_0 ratio. This finding was attributed to increase of the beam bending stiffness. In order to evaluate the influence of non-linear material behavior on the fracture, the *J*-integral values calculated assuming linear-elastic material behavior were plotted also in Fig. 5 for comparison (the *J*-integral linear-elastic solution was derived by substituting of m_1 = 1 in the non-linear solution). It can be observed in Fig. 5 that material non-linearity leads to increase of the *J*-integral value. Therefore, the non-linear material behavior has to be considered in fracture mechanics based safety design of functionally graded structural members.

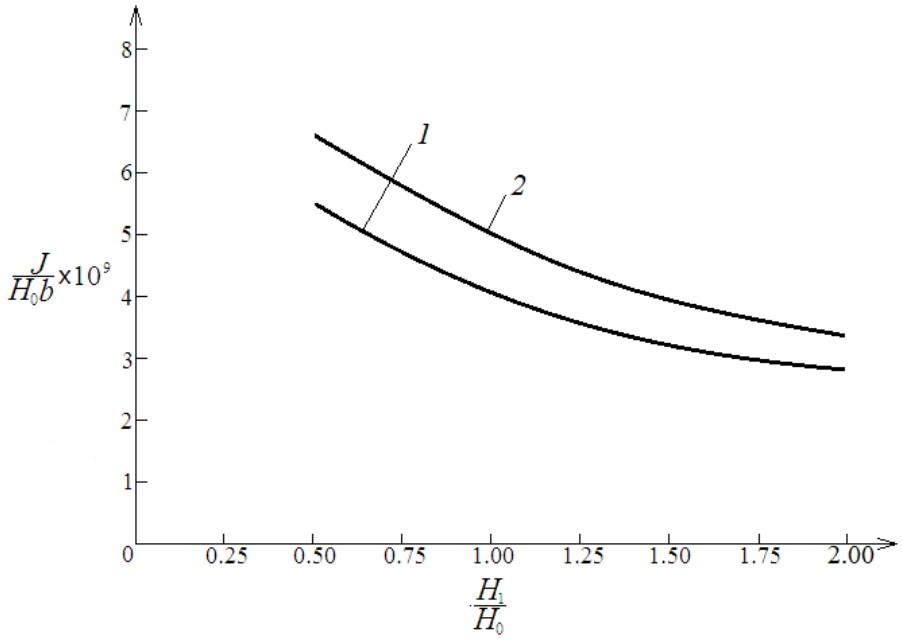

Fig. 5 The *J*-integral value (in non-dimensional form) plotted against H_1/H_0 ratio for $h_1/2h$ = 0.5 (curve 1 – linear-elastic material behavior, curve 2 – non-linear material behavior)

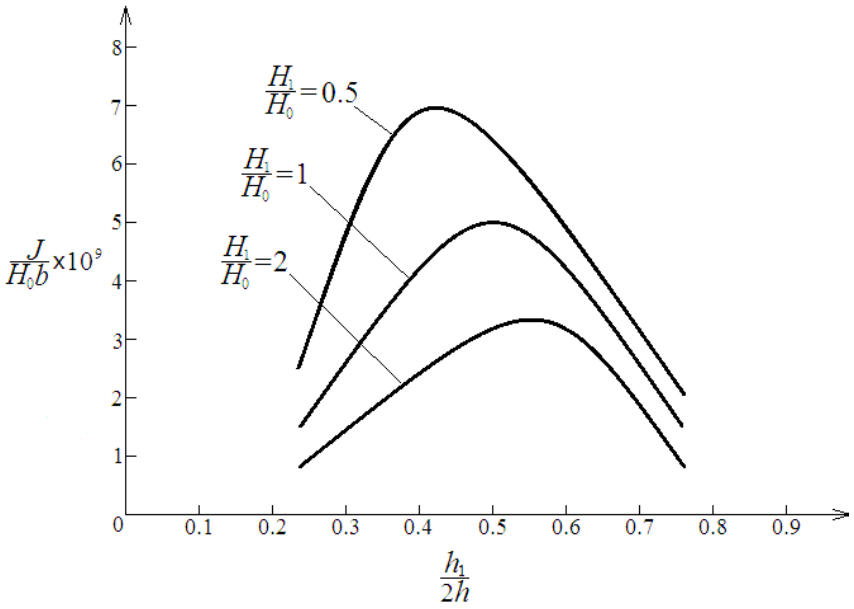

Fig. 6 The J-integral value (in non-dimensional form) as a function of crack location, $h_1/2h$, for material gradient of $H_1/H_0 = 0.5$, 1 and 2

Influence of the crack position along the beam height on the non-linear fracture was analyzed too (the crack position was characterized by $h_1/2h$ ratio (refer to Fig. 1)). The variation of J-integral value as a function $h_1/2h$ ratio for material gradient of $H_1/H_0 = 0.5$, 1 and 2 is shown in Fig. 6. The curves in Fig. 6 indicate that that the J-integral value is maximal when the crack is positioned near the mid-plane of ELS beam. The maximum of J-integral is exactly at $h_1/2h = 0.5$, when $H_1/H_0 = 1$, i.e., when the beam is homogeneous.

4. Conclusions

Mode II delamination fracture in the ELS functionally graded beam configuration was analyzed theoretically with taking into account the non-linear material behavior. For this purpose, the J-integral approach was applied. An analytical solution of the J-integral was derived assuming that the material is functionally graded transversally to the beam, i.e., along the beam height. Equations were obtained for crack arms curvature that was used in the J-integral solution. It was assumed that the ELS functionally graded beam mechanical response can be modeled analytically by using a power-law stress-strain relation (linear variation was assumed of the coefficient in the power-law stress-strain relation along the beam height). The non-linear solution derived is valid for a delamination crack located arbitrary along the beam height. In order to verify the J-integral non-linear solution, the strain energy release rate was analyzed with considering the material non-linearity. The influence of material gradient on the fracture behavior was evaluated. The analysis revealed that the J-integral value decreases with increasing H_1/H_0 ratio (H_0 and H_1 are the values of coefficient in the power-law stress-strain relation in the upper and lower edge of beam, respectively (refer to Eq. (4))). Concerning the influence of material non-linearity on the fracture behavior, the results of study indicate that the J-integral value increases when the material non-linearity is taken into account. This fact indicates that the non-linear material behavior has to be considered in fracture mechanics based safety deign of functionally graded structural members. The effect of crack position on the fracture was investigated too. It was found that the J-integral has highest value when the crack is positioned near the beam mid-plane. The analysis presented here is very suitable for parametric investigations, because the solution derived captures the essential of non-linear fracture. The analytical approach developed in the present paper can be used for optimization of functionally graded beam structures with respect to the fracture performance. The present study contributes also for a better understanding of delamination fracture under mode II crack loading conditions in functionally graded beam structures with material non-linearity.

Acknowledgments

Mode II delamination fracture in the ELS functionally graded beam configuration was analyzed theoretically with taking into account the non-linear material behavior. For this purpose, the J-integral approach was applied. An analytical solution of the J-integral was derived assuming that the material is functionally graded transversally to the beam, i.e., along the beam height. Equations were obtained for crack arms curvature that was used in the J-integral solution. It was assumed that the ELS functionally graded beam mechanical response can be modeled analytically by using a power-law stress-strain relation (linear variation was assumed of the coefficient in the power-law stress-strain relation along the beam height). The non-linear solution derived is valid for a delamination crack located arbitrary along the beam height. In order to verify the J-integral non-linear solution, the strain energy release rate

was analyzed with considering the material non-linearity. The influence of material gradient on the fracture behavior was evaluated. The analysis revealed that the *J*-integral value decreases with increasing H_1/H_0 ratio (H_0 and H_1 are the values of coefficient in the power-law stress-strain relation in the upper and lower edge of beam, respectively (refer to Eq. (4))). Concerning the influence of material non-linearity on the fracture behavior, the results of study indicate that the *J*-integral value increases when the material non-linearity is taken into account. This fact indicates that the non-linear material behavior has to be considered in fracture mechanics based safety deign of functionally graded structural members. The effect of crack position on the fracture was investigated too. It was found that the *J*-integral has highest value when the crack is positioned near the beam mid-plane. The analysis presented here is very suitable for parametric investigations, because the solution derived captures the essential of non-linear fracture. The analytical approach developed in the present paper can be used for optimization of functionally graded beam structures with respect to the fracture performance. The present study contributes also for a better understanding of delamination fracture under mode II crack loading conditions in functionally graded beam structures with material non-linearity.

References

Ahouel, M., Houari, M., Bedia, E. and Tounsi, A. (2016), "Size-dependent mechanical behaviour of functionally graded trigonometric shear deformation nanobeams including neutral surface position concept", *Steel Compos. Struct., Int. J.*, **20**(5), 963-981.

Akbas, S. (2015), "Wave propagation of a functionally graded beam in thermal environments", *Steel Compos. Struct., Int. J.*, **19**(6), 1421-1447.

Anlas, G., Santare, M.H. and Lambros, J. (2000), "Numerical calculation of stress intensity factors in functionally graded materials", *Int. J. Fracture*, **104**(1), 131-143.

Atmane, H., Tounsi, A., Bernard, F. and Mahmoud, S. (2015), "A computational shear model for vibrational analysis of functionally graded beams with porosities", *Steel Compos. Struct., Int. J.*, **19**(2), 369-385.

Bedia, A. and Bousahla, A. (2016), "Mechanical and hydrothermal behaviour of functionally graded plates using a hyperbolic shear deformation theory", *Steel Compos. Struct., Int. J.*, **20**(4), 889-912.

Benferhat, R., Daouadji, T., Hadji, L. and Said Mansour, M. (2016), "Static analysis of the FGM plate with porosities", *Steel Compos. Struct., Int. J.*, **21**(1), 123-136.

Bennai, R., Atmabe, H. and Tounsi, A. (2015), "A new higher-order shear and normal deformation theory for functionally graded sandwich beams", *Steel Compos. Struct., Int. J.*, **19**(3), 521-546.

Bohidar, S.K., Sharma, R. and Mishra, P.R. (2014), "Functionally graded materials: A critical review", *Int. J. Res.*, **1**(7), 289-301.

Bounouara, F., Benrahou, K., Belkorissat, I. and Tounsi, A. (2016), "A nonlocal zeroth-order shear deformation theory for free vibration of functionally graded nanoscale plates resting on elastic foundation", *Steel Compos. Struct., Int. J.*, **20**(2), 227-249.

Carpinteri, A. and Pugno, N. (2006), "Cracks in re-entrant corners in functionally graded materials", *Eng. Fracture Mech.*, **73**(6), 1279-1291.

Chakrabarty, J. (2006), *Theory of Plasticity*, Elsevier Butterworth-Heinemann, Oxford, UK.

Darlimaz, K. (2015), "Vibration analysis of functionally graded material (FGM) grid system", *Steel Compos. Struct., Int. J.*, **18**(2), 395-408.

Galeban, M., Mojahedin, A., Taghavi, Y. and Jabbari, M. (2016), "Free vibration of functionally graded thin beams made of saturated porous materials", *Steel Compos. Struct., Int. J.*, **21**(5), 999-1016.

Kaman, M.O. and Cetisli, F. (2012), "Numerical analysis of center cracked orthotropic fgm plate: Crack and material axes differ by θ°", *Steel Compos. Struct., Int. J.*, **13**(2), 187-206. DOI: 10.12989/scs.2012.13.2.187

Lubliner, J. (2006), *Plasticity Theory* (Revised Edition), University of California, Berkeley, CA, USA.

Parvanova, S.L., Dineva, P.S. and Manolis, G.D. (2013), "Dynamic behavior of a finite-sized elastic solid with multiple cavities and inclusions using BIEM", *Acta Mech.*, **224**, 597-618.

Parvanova, S.L., Dineva, P.S., Manolis, G.D. and Kochev, P.N. (2014), "Dynamic response of a solid with multiple inclusions under anti-plane strain conditions by the BEM", *Comput. Struct.*, **139**, 65-83.

Pei, G. and Asaro, R.J. (1997), "Cracks in functionally graded materials", *Int. J. Solids Struct.*, **34**(1), 1-17.

Petrov, V.V. (2014), *Non-linear Incremental Structural Mechanics*, M.: Infra-Injeneria.

Rajabi, M., Soltani, N. and Eshraghi, I. (2016), "Effects of temperature dependent material properties on mixed mode crack tip parameters of functionally graded materials", *Struct. Eng. Mech., Int. J.*, **58**(2), 217-230. DOI: 10.12989/sem.2016.58.2.217

Szekrenyes, A. (2012), "J-integral for delaminated beam and plate models", *Periodica polytechnica, Mech. Eng.*, **56**(1), 63-71.

Tilbrook, M.T., Moon, R.J. and Hoffman, M. (2005), "Crack propagation in graded composites", *Compos. Sci. Technol.*, **65**(2), 201-220.

Upadhyay, A.K. and Simha, K.R.Y. (2007), "Equivalent homogeneous variable depth beams for cracked FGM beams; compliance approach", *Int. J. Fract.*, **144**(2), 209-213.

Uslu Uysal, M. (2017), "Virtual crack closure technique on delamination fracture toughness of composite materials based on epoxy resin filled with micro-scale hard coal", *Acta Physica Polonica A*. [In press]

Uslu Uysal, M. and Güven, U. (2016), "A bonded plate having orthotropic inclusion in adhesive layer under in-plane shear loading", *J. Adhesion*, **92**(3), 214-235. DOI: 10.1080/00218464.2015.1019064

Uslu Uysal, M. and Kremzer, M. (2015), "Buckling behaviour of short cylindrical functionally gradient polymeric materials", *Acta Physica Polonica A*, **127**(4), 1355-1357. DOI: 10.12693/APhysPolA.127.1355

Uysal, M. (2016), "Buckling behaviours of functionally graded polymeric thin-walled hemispherical shells", *Steel Compos. Struct., Int. J.*, **21**(4), 849-862.

Zhang, H., Li, X.F., Tang, G.J. and Shen, Z.B. (2013), "Stress intensity factors of double cantilever nanobeams via gradient elasticity theory", *Eng. Fract. Mech.*, **105**(1), 58-64.

CC